Journal of Applied Polymer Science

Fabrication of a poly(ε-caprolactone)/starch nanocomposite scaffold with a solvent-casting/salt-leaching technique for bone tissue engineering applications

Safa Taherkhani, Fathollah Moztarzadeh
Department of Biomedical Engineering (Center of Excellence), Amirkabir University of Technology, P. O. Box 15875-4413, Tehran, Iran
Correspondence to: F. Moztarzadeh (E-mail: moztarzadeh@aut.ac.ir)

ABSTRACT: A series of nanocomposite scaffolds of poly(ε-caprolactone) (PCL) and starch with a range of porosity from 50 to 90% were fabricated with a solvent-casting/salt-leaching technique, and their physical and mechanical properties were investigated. X-ray diffraction patterns and Fourier transform infrared spectra confirmed the presence of the characteristic peaks of PCL in the fabricated scaffolds. Microstructure studies of the scaffolds revealed a uniform pore morphology and structure in all of the samples. The experimental measurements showed that the average contact angle of the PCL/starch composite was 88.05 ± 1.77°. All of the samples exhibited compressive stress/strain curves similar to those of polymeric foams. The samples with 50, 60, 70, and 80 wt % salt showed compressive-load-resisting capabilities in the range of human cancellous bone. With increasing porosity, a significant decrease in the mechanical properties of the scaffolds was observed. © 2016 Wiley Periodicals, Inc. J. Appl. Polym. Sci. **2016**, *133*, 43523.

KEYWORDS: biomaterials; composites; mechanical properties; polyesters; porous materials

Received 15 August 2015; accepted 6 February 2016
DOI: 10.1002/app.43523

INTRODUCTION

Bone tissue engineering is a main research area of regenerative medicine field. Although the self-healing of a critical size bone defect is difficult, a foreign porous material used to support and promote cellular activity is very helpful.[1] One of the major challenges now facing bone tissue engineering is the need for three-dimensional scaffolds that offer a local microenvironment for cell migration and proliferation.[2–4] In addition to adequate physical and biological properties, these scaffolds should present appropriate mechanical behavior in a highly porous structure.[5]

Biodegradable synthetic polymers, such as polyesters, are now being used as promising materials for bone tissue engineering scaffolds.[6–8] In addition to their great mechanical properties, polyesters offer a number of advantages over other materials. For example, they have the ability to be fabricated into various shapes with desired pore architectures and morphologies.

Among the aliphatic polyester family, poly(ε-caprolactone) (PCL) is one of the most excellent biocompatible and biodegradable polymers; it has outstanding processability because of its low melting point and good solubility in organic solvents.[9] PCL dissolves in acetone, tetrahydrofuran, chloroform, methylene chloride, dimethylformamide (DMF), acetic acid, and formic acid.[10–14]

A number of processing techniques, including salt/particulate leaching, gas foaming, electrospinning, freeze drying, and solid freeform, have been used to fabricate PCL scaffolds with adequate mechanical properties.[12,14–17] One of the most conventional techniques used to fabricate porous three-dimensional scaffolds of PCL is solvent casting/salt leaching. This technique has shown great capability for controlling the porosity, pore size, and pore morphology of scaffolds. These parameters are directly dependent on the proportion, size, and shape, respectively, of the porogen particles.[18] Other advantages of the solvent-casting/salt-leaching technique include its simplicity and low cost compared to other conventional techniques.

The solvent-casting/salt-leaching technique consists of four steps: (1) the homogeneous dispersion of porogen particles in a polymer solution, (2) the pouring of the obtained mixture into the mold, (3) the removal of the solvent from solution via evaporation, and (4) the immersion of the polymer/salt composite in water or a proper solvent to leach out the porogen particles.[12] Various kind of salts, such as sodium chloride (NaCl), sodium bicarbonate, sodium acetate, and saccharose, have been used as porogen agents.[12,13,19–21]

In addition to its simplicity, the solvent-casting/salt-leaching method is associated with some challenges. For example, the

mechanism of removing the solvent from the polymeric solution may lead to dimensional shrinkage or the trapping of the solvent inside the samples. Previous publications have mentioned that solvent casting/salt leaching is a suitable technique for producing membranes, wafers, or thin scaffolds up to 3 mm only.[22]

As mentioned previously, the porosity and mechanical strength are two main properties that are required for the successful production of bone scaffolds for use in in load-bearing applications. Bulk PCL presents compression moduli in the range 330–360 MPa.[23] Some previous studies were performed to prepare porous PCL scaffolds with a microstructure and mechanical properties close to those of human cancellous bone (pore size = 100–500 μm, porosity = 50–90%, compressive strength = 1.5–9.3 MPa, Young's modulus = 100–400 MPa).[24] Results show that the compression modulus of the porous PCL scaffolds decreased from 8.15 MPa the scaffolds with a 60% porosity to less than 0.l MPa for scaffolds with a 90% porosity.[13,25,26]

In this study, we aimed to design and fabricate a three-dimensional architecture of PCL with a microstructure and mechanical properties close to those of human cancellous bone. The solvent-casting/salt-leaching technique was applied to prepare a series of PCL scaffolds with different porosities. NaCl with various particle size distributions was used as a porogen agent. To improve the biodegradability and hydrophilicity of the scaffolds and to create nanopores, starch nanopowder was added to the polymeric solution. Finally, the physical and mechanical properties of the obtained scaffolds were investigated.

EXPERIMENTAL

Materials

PCL, with a molecular weight in the range 70,000–80,000 Da, was purchased from Sigma Aldrich. NaCl was used as the porogen agent to create a highly porous structure with an interconnected pore network. Because the optimum pore size for promoting bone ingrowth is in the range 100–500 μm,[24] the particle size distribution of salt was considered to be in this range. Extrapure salt was milled and passed through 40-, 50-, 60-, and 170-mesh standard sieves in sequence. The weight percentages of the powder salt in each mesh size were 20, 20, 30, and 30, respectively. Starch nanopowder and all organic solvents were purchased from Merck Chemical Co.

Preparation of the PCL/Starch Nanocomposite Scaffolds

The preparation of the PCL/starch nanocomposite scaffolds with the solvent-casting/salt-leaching technique can be summed up as follows: PCL was dissolved in a chloroform/DMF binary solvent system. The starch nanopowder was dispersed in a small amount of solvent with the aid of an ultrasonic bath. The obtained mixture was added to the polymeric solution, and the whole system was stirred for 1 h. The total volume of solvent used for dissolving PCL and dispersing the starch nanopowder was 12 cm^3. The weight ratio of starch to PCL was set at 1:9. The total amount of solid materials including PCL and starch was 2 g. Sieved NaCl was added to the solution, and the suspension was continuously stirred until the viscosity increased. The final mixture was cast into cylindrical Teflon molds. To control the rate of solvent evaporation, the molds were covered with a perforated aluminum sheet. The samples were left for 72 h until the solvent was completely removed. Finally, the salt was washed out through the immersion of the samples in deionized water for 2 days. We obtained a constant weight of the wet samples after 2 days, and this confirmed that the salt was completely leached out from the samples. The salt-removed samples were then dried in an incubator at 37 °C.

Table I. Sample Compositions and Percentages of NaCl Used as a Porogen Agent

Sample	PCL (wt %)	Starch (wt %)	NaCl (wt %)
S0	90	10	0
S50	45	5	50
S60	36	4	60
S70	27	3	70
S80	18	2	80
S90	9	1	90

Five series of polymeric scaffolds with different porosities and a densities (without porosity) were prepared through changes in the percentage of salt, as reported in Table I.

Characterization of the PCL/Starch Nanocomposite Scaffolds

The surface morphology and microstructure of the polymeric scaffolds were investigated with a Philips XL30 scanning electron microscope. To determine the structural analysis of the samples, X-ray diffraction (XRD) analysis was performed with an Inel X-ray diffractometer (model Equinox 2000). For qualitative analysis, XRD diagrams were recorded in the interval $10^\circ \leq 2\theta \leq 90^\circ$ at a scan speed of 2°/min. The samples were also characterized by Fourier transform infrared (FTIR) spectroscopy with a Bruker Alpha spectrophotometer.

The hydrophilicity of the samples was evaluated by water contact angle measurements performed on a contact angle system (Dataphysics OCA 15 plus). A water droplet was poured on the surface of samples, and the water contact angle was measured after 3 s. Three measurements were recorded, and the results were expressed as averages and standard deviations.

The apparent porosities of the samples were measured according to ASTM C134.[27] The dry samples were weighed and immersed in deionized water for 2 h. After we measured the suspended weight, the samples were taken out and wiped with moistened cotton until all drops of water were removed from the surface. Then the saturated weights of the samples were determined. The apparent porosity (P_a) was calculated with the following equation:

$$P_a(\%) = (S-D)/(S-I) \times 100$$

where S is the saturated weight of the sample, D is the dried weight of the sample, and I is the immersed weight of the sample.

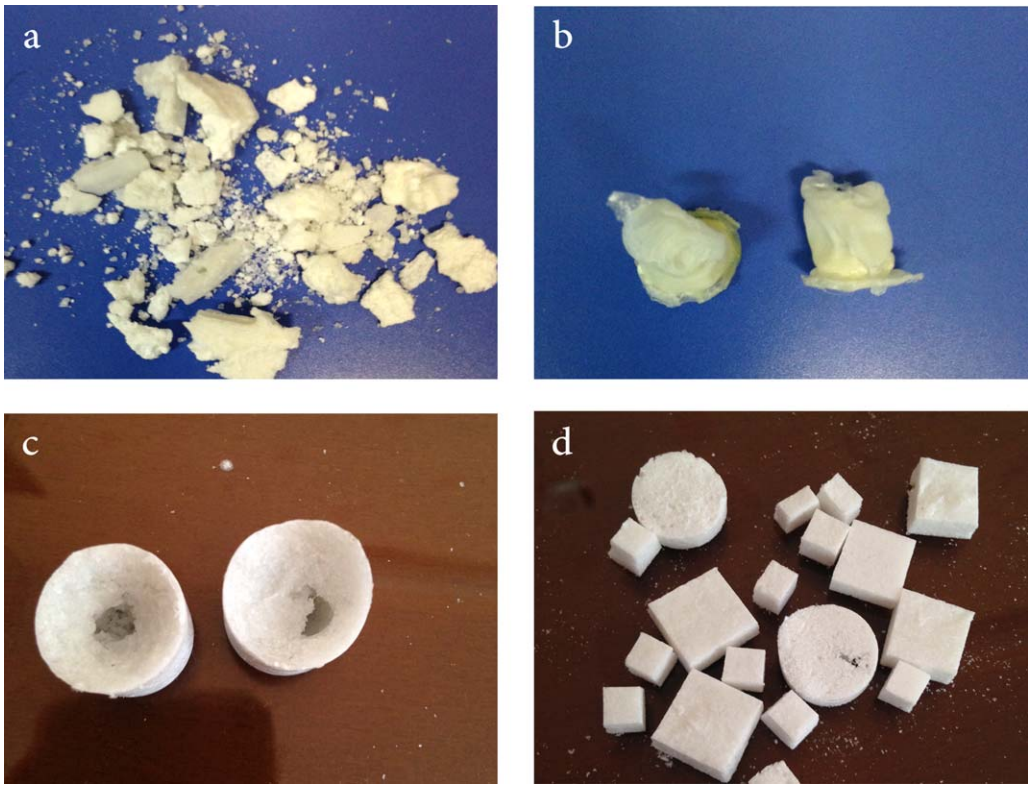

Figure 1. Photographs of specimens prepared via the solvent-casting method with (a) acetic acid/formic acid, (b) acetone, (c) chloroform, and (d) chloroform/DMF. [Color figure can be viewed in the online issue, which is available at wileyonlinelibrary.com.]

The compressive mechanical properties of the samples were measured according to ASTM D695-02a[28] by a dynamic testing machine (HCT 400/25, Zwick/Roell, Germany). For each sample, three cubic specimens ($5 \times 5 \times 5\,mm^3$) were compressed at a rate of 1 mm/min until the thickness decreased to 10% of its initial height. The modulus of elasticity, or Young's modulus, was determined as the slope of the elastic region, and the compressive strength was defined by the maximum on the curve just after the elastic region. The results are presented as the average values of three measurements and standard deviations.

RESULTS AND DISCUSSION

Despite its simplicity, the solvent-casting method involves the consideration of several critical factors, such as the type of solvent, rate of solvent evaporation, concentration and viscosity of the polymer solution, porogen type and size, and casting parameters.[29] These factors can strongly affect the physical and mechanical behavior of scaffolds. For example, the evaporation of the solvent plays an important role in the shape and strength of the obtained specimens. High solvent evaporation rates may cause dimensional shrinkage and body deformation.

In this study, to determine an optimum solvent system for the solvent casting of PCL, different single-solvent and binary solvent systems, including chloroform, DMF, acetone, acetic acid, and formic acid, were studied. The experiments were performed several times with various amounts of solvents. In all experiments, the weight ratio of starch to PCL was constant at 1:9. For better comparison, the experiments were repeated with and without salt. Figure 1 shows photos of the samples prepared with different solvent systems. Although acetic acid and formic acid are the most commonly used solvents for electrospinning PCL,[14,30] the samples prepared with these suffered from poor solidity [Figure 1(a)], so they were easily broken or crushed during handling. In the samples dissolved by acetone (boiling point = 56 °C), the rapid evaporation of the solvent induced shrinkage and three-dimensional deformation [Figure 1(b)].

In the samples dissolved by chloroform (boiling point = 61 °C), the evaporation of solvent from the surface resulted in trapped vapor under the solidified surfaces and the creation of holes [Figure 1(c)], although the samples prepared by chloroform showed a higher mechanical strength than the others did.

The use of DMF (boiling point = 153 °C) as a solvent caused less body deformation in the specimens; however, some residual solvent remained in the samples because of the low evaporation rate of DMF.

We determined experimentally that the use of a combination of chloroform and DMF led to a better result. The best result was obtained when a mix of chloroform and DMF at a volume ratio of 6:1 was used. When two solvents are mixed, their combined boiling point is somewhere between the two separate boiling points and is usually correlated with the partial molar fraction of each.[31] Therefore, mixture with chloroform increased the chance for DMF to be removed from the samples. Furthermore, the use of DMF as a cosolvent led to the suppression of the

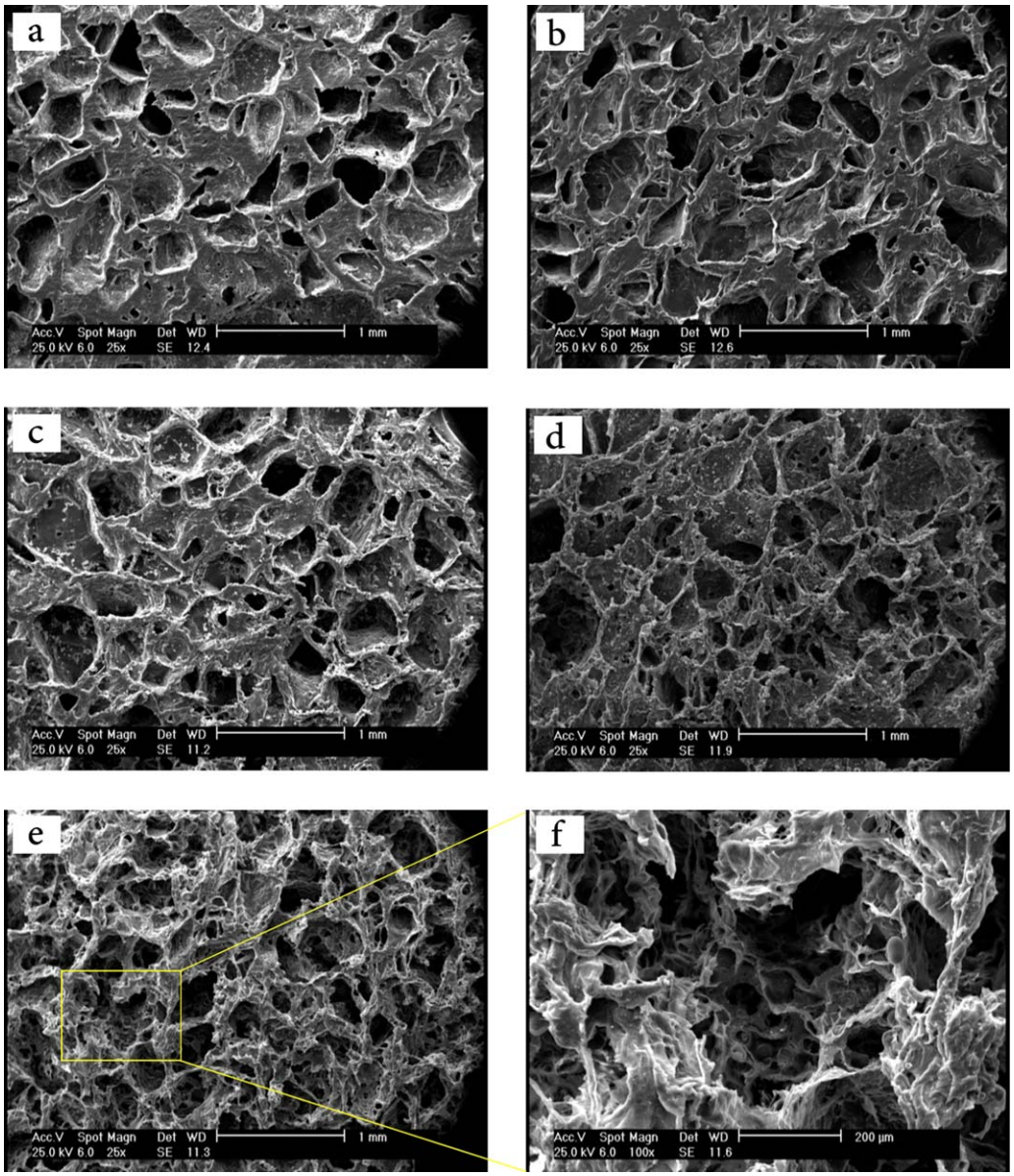

Figure 2. SEM micrographs of the samples: (a) Sr0, (b) Sr50, (c) Sr60, (d) Sr70, (e) Sr80, (e) Sr90 at low magnification (25×), and (f) Sr90 at a high magnification (100×). [Color figure can be viewed in the online issue, which is available at wileyonlinelibrary.com.]

rapid evaporation of chloroform. When we controlled the evaporation rate of the solvent, the samples presented the minimum defects in their shape and body [Figure 1(d)].

The pore size distribution, porosity, and pore interconnectivity of scaffolds should be adequate for cell migration, matrix deposition, vascularization, and mass transport of nutrients from and to cells.[32] Scanning electron microscopy (SEM) of the cross sections of five three-dimensional scaffolds revealed uniform pore morphologies and structures in all of the samples (Figure 2). As expected, when the salt amount was increased, the porosity of the samples increased considerably, whereas the wall thickness, defined as the distance between neighboring pores, decreased. The samples exhibited a sponge structure with interconnected pores.

The SEM micrograph also confirmed that the pores size of the scaffolds differed from 50 to 500 μm. The pore size distribution was in accordance with the size of the salt that was used to provide pore sizes in the range 88–420 μm, although the salt was not the only origin of the pores. Removal of the remaining

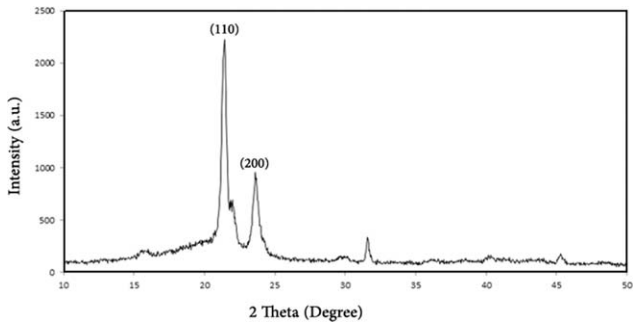

Figure 3. XRD pattern of the PCL/starch nanocomposite.

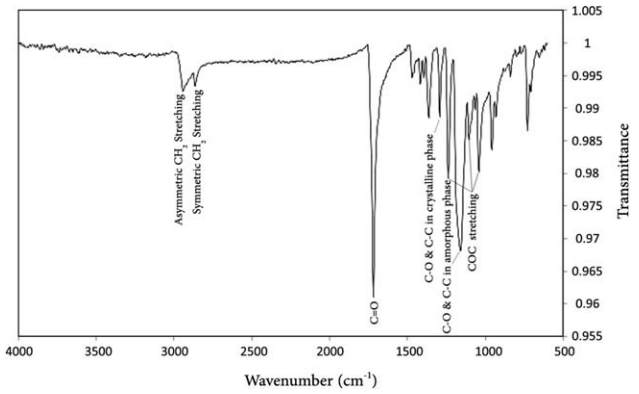

Figure 4. FTIR spectra of the PCL/starch composite.

solvent and/or dissolution of the starch in water created additional pores.

The high-magnification (100×) SEM image clearly demonstrated a hierarchical pore structure with interconnected pores of different dimensions in the sample S90 (the sample within 90% salt), which is shown in the selected area in the yellow square frame [Figure 2(f)].

Figure 3 shows the XRD pattern of the PCL/starch nanocomposite. The composite exhibited two strong diffraction peaks at 21.42 and 23.61°; these were related to the (110) and (200) planes, respectively, of PCL.[33]

The FTIR spectra of the samples confirmed the presence of characteristic peaks of PCL in the composite (Figure 4). The bands appearing at 2941 and 2864 cm^{-1} were assigned to asymmetric and symmetric CH_2 stretching, respectively. The characteristic band of PCL at 1719 cm^{-1} was attributed to the C═O stretching of the ester carbonyl group. The bands at 1292 and 1159 cm^{-1} were ascribed to C—O and C—C stretching in the crystalline and amorphous phases, respectively. The bands at 1237, 1105, and 1042 cm^{-1} were attributed to COC stretching.[34–37]

Surface wettability is a consequential physicochemical property of biomaterials and can influence cellular affinity to them. PCL possesses a hydrophobic nature (caused by five continuous methyl groups); this results in a lower degradation rate among other polyesters. Studies have shown that pure PCL takes more

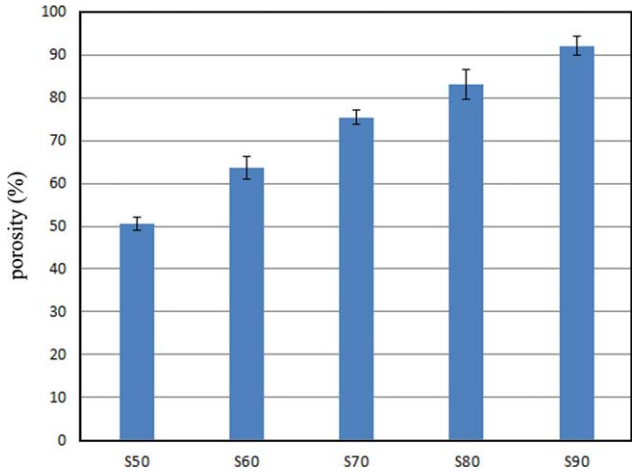

Figure 6. Apparent porosity of the scaffolds. [Color figure can be viewed in the online issue, which is available at wileyonlinelibrary.com.]

than 2 years to degrade completely.[38] This weakness may also lead to a reduction in the cellular affinity to scaffolds made by PCL and may discourage cellular activities such as adhesion and migration. The use of different techniques, such as surface modification or blending with other polymers, can improve the degradation behavior and biological properties of PCL. Figure 5 displays the water contact angle for the membranes prepared from the PCL/starch nanocomposites. The average contact angle for the nanocomposite composed of 90 wt % PCL and 10 wt % starch was 88.05 ± 1.77°.

The apparent porosity shows the ratio of the open pore volume to the specimen volume (Figure 6). The results of the measured porosity were approximately in accordance with the percentage of salt that was initially used to create pores. For example, the measured porosity of S50 (the sample with 50% salt) was 50.58 ± 1.46%, and the measured porosity of S70 (the sample with 70% salt) was 75.40 ± 1.75%. However, the experimental data shows that the porosity of the samples was slightly higher than what was expected from the complete elimination of the salt porogen. Removal of the remaining solvent and/or the dissolution of the starch in water created additional pores.

The compressive stress/strain curves of the samples are shown in Figure 7. All of the curves exhibited characteristics similar to

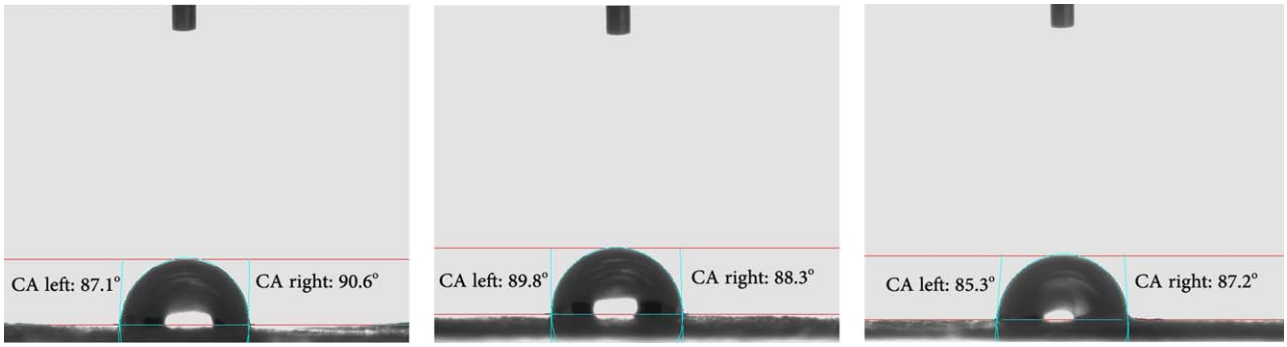

Figure 5. Water contact angle (CA) for the three membranes prepared from the PCL/starch nanocomposite. [Color figure can be viewed in the online issue, which is available at wileyonlinelibrary.com.]

those of polymeric foams under compressive loading, which were defined by the absence of a yield point maximum but exhibited a plateau in the stress/strain curve. This behavior often presents a large recoverable strain at low stress levels and a terminal increase in the stress followed by failure; this leads to a tear with little permanent deformation in the failure surface.[13,39,40] As shown in Figure 7, at the beginning of each curve, a linear elastic region appeared, and right after that, there was a region where the stress steeply increased at very small strain.

To study the mechanical properties of scaffolds, the mechanical behavior of natural bone, such as its elastic modulus, compressive strength, and tensile strength, must be considered. Human cancellous bone has a compressive strength in the range 1.5–9.3 MPa and a Young's modulus in the range 100–400 MPa.[24]

Table II shows the mean values of Young's modulus and the compressive strength of each sample. The dense sample had a Young's modulus of 32.06 ± 2.74 MPa and a compressive strength of 19.45 ± 1.94 MPa. With increasing porosity, a significant diminution in the compressive properties of the scaffolds was observed. S50 (the sample with $50.58 \pm 1.46\%$ porosity), S60 (the sample with $63.46 \pm 2.58\%$ porosity), S70 (the sample with $75.40 \pm 1.75\%$ porosity), and S80 (the sample with $83.19 \pm 3.50\%$ porosity) showed compressive-load-resisting capabilities in the range of human cancellous bone. The Young's moduli of all of the samples were found to be less than that of human cancellous bone.

Polymers by themselves are generally flexible and exhibit a low mechanical strength and stiffness, whereas inorganic materials, such as bioceramics, are known to be stiff and brittle. Because of the inherently higher stiffness and strength of bioceramics, their combination with biopolymers leads to composite materials with improved mechanical properties. On the other hand, the longevity of mechanical properties during the degradation process has a significant effect on scaffold performance. Although the polymer matrix is degrading, the three-dimensional scaffold must provide physical support until the engineered tissue has adequate mechanical integrity to support itself. It is mandatory for successful tissue regeneration to control the degradation time profile of the scaffold at the defect site.[41–43]

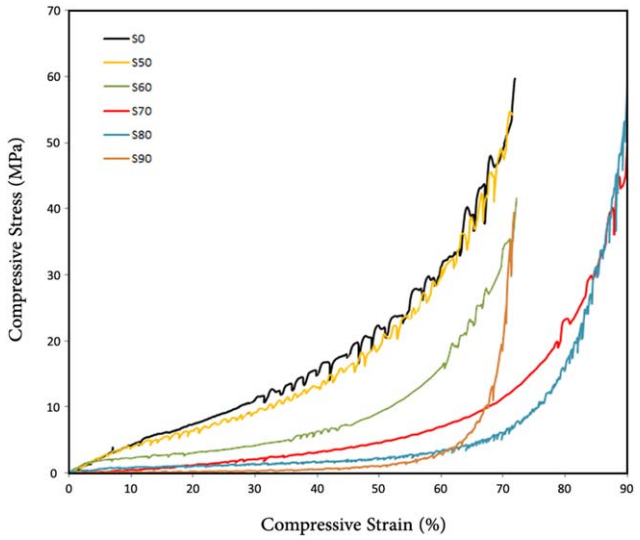

Figure 7. Compressive stress/strain curves of the samples. [Color figure can be viewed in the online issue, which is available at wileyonlinelibrary.com.]

Table II. Compressive Mechanical Properties of the Specimens and Human Cancellous Bone

	Measured porosity (%)	Young's modulus (MPa)	Compressive strength (MPa)
Human cancellous bone	50–90	100–400	1.5–9.3
S0		32.06 ± 2.74	19.45 ± 1.94
S50	50.58 ± 1.46	26.08 ± 1.72	13.68 ± 1.39
S60	63.46 ± 2.58	19.05 ± 1.70	10.78 ± 0.93
S70	75.40 ± 1.75	6.62 ± 0.67	2.48 ± 0.39
S80	83.19 ± 3.50	3.92 ± 0.11	1.68 ± 0.18
S90	92.13 ± 2.12	1.73 ± 0.23	0.67 ± 0.09

In this study, we designed and fabricated a three-dimensional architecture of PCL as a high potential material for bone tissue engineering scaffolds. Future studies would benefit from the addition of bioceramics such as bioactive glasses into the polymeric matrix to improve the initial mechanical properties and the mechanical properties during the degradation process.

CONCLUSIONS

A series of nanocomposite scaffolds of PCL and starch with a range of porosities from 50 to 90% were fabricated with a solvent-casting/salt-leaching technique. The obtained scaffolds exhibited suitable porosity, pore size, and pore interconnectivity as well as adequate mechanical properties for bone tissue engineering applications. The results of this study show that PCL has a great potential to produce highly porous scaffolds with a solvent-casting/salt-leaching technique.

ACKNOWLEDGMENTS

The authors thank Khadijeh Fallahmorad for her assistance and hard work.

REFERENCES

1. Pina, S.; Oliveira, J. M.; Reis, R. L. *Adv. Mater.* **2015**, *27*, 1143.
2. Sezer, U. A.; Arslantunali, D.; Aksoy, E. A.; Hasirci, V.; Hasirci, N. *J. Appl. Polym. Sci.* **2014**, *131*, 40110.
3. Anitha, A.; Sowmya, S.; Sudheesh Kumar, P. T.; Deepthi, S.; Chennazhi, K. P.; Ehrlich, H.; Tsurkan, M.; Jayakumar, R. *Prog. Polym. Sci.* **2014**, *39*, 1644.

4. Mozafari, M.; Gholipourmalekabadi, M.; Chauhan, N. P. S.; Jalali, N.; Asgari, S.; Caicedoa, J. C.; Hamlekhan, A.; Urbanska, A. M. *Mater. Sci. Eng. C* **2015**, *50*, 117.
5. Abedalwafa, M.; Wang, F.; Wang, L.; Li, C. *Mater. Sci.* **2013**, *34*, 123.
6. Boccaccini, R.; Gough, J. E. Tissue Engineering Using Ceramics and Polymers; Woodhead: Cambridge, England, **2007**.
7. Hollander, A. P.; Hatton, P. V. Biopolymer Methods in Tissue Engineering; Methods in Molecular Biology 238; Humana: New York, **2004**.
8. Shadjou, N.; Hasanzadeh, M. *Mater. Sci. Eng. C.* **2015**, *55*, 401.
9. Woodruff, M. A.; Hutmacher, D. *W. Prog. Polym. Sci.* **2010**, *35*, 1217.
10. Pasquale, N. D.; Marchisio, D. L.; Barresi, A. A.; Carbone, P. *J. Phys. Chem. B* **2014**, *118*, 13258.
11. Yang, Q.; Chen, L.; Shen, X.; Tan, Z. *J. Macromol. Sci. Phys.* **2006**, *45*, 1171.
12. Cannillo, V.; Chiellini, F.; Fabbri, P.; Sola, A. *Compos. Struct.* **2010**, *92*, 1823.
13. Reignier, J.; Huneault, M. A. *Polymer* **2006**, *47*, 4703.
14. Van der Schueren, L.; Steyaert, I.; De Schoenmaker, B.; De Clerck, K. *Carbohydr. Polym.* **2012**, *88*, 1221.
15. Lim, Y. M.; Gwon, H. J.; Shin, J.; Pyo Jeun, J.; *Chang Nho, Y. J. Ind. Eng. Chem.* **2008**, *14*, 436.
16. Yang, G. H.; Kim, M.; Kim, G. H. A. J. *Colloid Interface Sci.* **2015**, *450*, 159.
17. Gaudio, C. D.; Ercolani, E.; Nanni, F.; Bianco, A. *Mater. Sci. Eng. A* **2011**, *528*, 1764.
18. Mano, J. F.; Silva, G. A.; Azevedo, H. S.; Malafaya, P. B.; Sousa, R. A.; Silva, S. S.; Boesel, L. F.; Oliviera, J. M.; Santos, T. C.; Marques, A. P.; Neves, N. M.; Reis, R. L. *J. R. Soc. Interface* **2007**, *4*, 999.
19. Han, D. K.; Ahn, K. D.; Kim, J. M.; Ju, Y. M. U.S. Patent 6,562,374 (**2003**).
20. Marcos, M.; Cano, P.; Fantazzini, P.; Garavaglia, C.; Gomez, S.; Garrido, L. *Magn. Reson. Imaging* **2006**, *24*, 89.
21. Liao, C. J.; Lin, Y. J.; Chen, C. F.; Chang, K. Y. U.S. Patent 6,824,716 (**2004**).
22. Moore, M. J.; Jabbari, E.; Ritman, E. L.; Lu, L. C.; Currier, B. L.; Windebank, A. J.; Yaszemski, M. J. *J. Biomed. Mater. Res. Part A* **2004**, *71*, 258.
23. Azevedo, M. C.; Reis, R. L.; Claase, B. M.; Grijpma, D. W.; Feijen, J. *J. Mater. Sci. Mater. Med.* **2003**, *14*, 103.
24. Alvarez, K.; Nakajima, H. *Materials* **2009**, *2*, 790.
25. Thadavirul, N.; Pavasant, P.; Supaphol, P. *J. Biomed. Mater. Res. Part A* **2014**, *102*, 3379.
26. Lebourg, M.; Sabater Serra, R.; Mas Estelles, J.; Hernandez Sanche, F.; Gomez Ribelles, J. L.; Suay Anton, J. *J. Mater. Sci. Mater. Med.* **2008**, *19*, 2047.
27. ASTM C134-95(2010). Standard Test Methods for Size, Dimensional Measurements, and Bulk Density of Refractory Brick and Insulating Firebrick; ASTM International: West Conshohocken, PA, **2010**.
28. ASTM D695-02a. Standard Test Method for Compressive Properties of Rigid Plastics; ASTM International: West Conshohocken, PA, **2002**.
29. Qin, L.; Genant, H. K.; Griffith, J. F.; Leung, K. S. Advanced Bioimaging Technologies in Assessment of the Quality of Bone and Scaffold Materials; Springer: New York, **2007**.
30. Shalumon, K. T.; Anulekha, K. H.; Girish, C. M.; Prasanth, R.; Nair, S. V.; Jayakumar, R. *Carbohydr. Polym.* **2010**, *80*, 413.
31. Ghosal, S. K.; Datta, S. Introduction to Chemical Engineering; Tata McGraw-Hill Education: Noida, India, **2011**.
32. Loh, Q. L.; Choong, C. *Tissue Eng. Part B Rev.* **2013**, *19*, 485.
33. Borjigin, M.; Eskridge, C.; Niamat, R.; Strouse, B.; Bialk, P.; Kmiec, E. B. *Int. J. Nanomed.* **2013**, *8*, 855.
34. Elzein, T.; Nasser-Eddine, M.; Delaite, C.; Bistac, S.; Dumas, P. J. *Colloid Interface Sci.* **2004**, *273*, 38.
35. Li, H.; Sivasankarapillai, G.; McDonald, A. G. *J. Appl. Polym. Sci.* **2014**, *131*, 41389.
36. Li, H.; Sivasankarapillai, G.; McDonald, A. G. *J. Appl. Polym. Sci.* **2015**, *132*, 41389.
37. Li, H.; Sivasankarapillai, G.; McDonald, A. G. *Ind. Crops Prod.* **2015**, *67*, 143.
38. Sun, H.; Mei, L.; Song, C.; Cui, X.; Wang, P. *Biomaterials* **2006**, *27*, 1735.
39. Mercier, J. P.; Zambelli, G.; Kurz, W. Introduction to Materials Science; Elsevier: Amsterdam, **2003**; Chapter 15.
40. Gibson, L. J.; Ashby, M. F. Cellular Solids, Structure and Properties; Pergamon: Oxford, **1988**.
41. Diba, M.; Kharaziha, M.; Fathi, M. H.; Gholipourmalekabadi, M.; Samadikuchaksaraei, A. *Compos. Sci. Technol.* **2012**, *72*, 716.
42. Wu, F.; Liu, C.; O'Neill, B.; Wei, J.; Ngothai, Y. *Appl. Surf. Sci.* **2012**, *258*, 7589.
43. McClure, M. J.; Simpson, D. J.; Bowlin, G. L. *J. Mech. Behav. Biomed. Mater.* **2012**, *10*, 48.